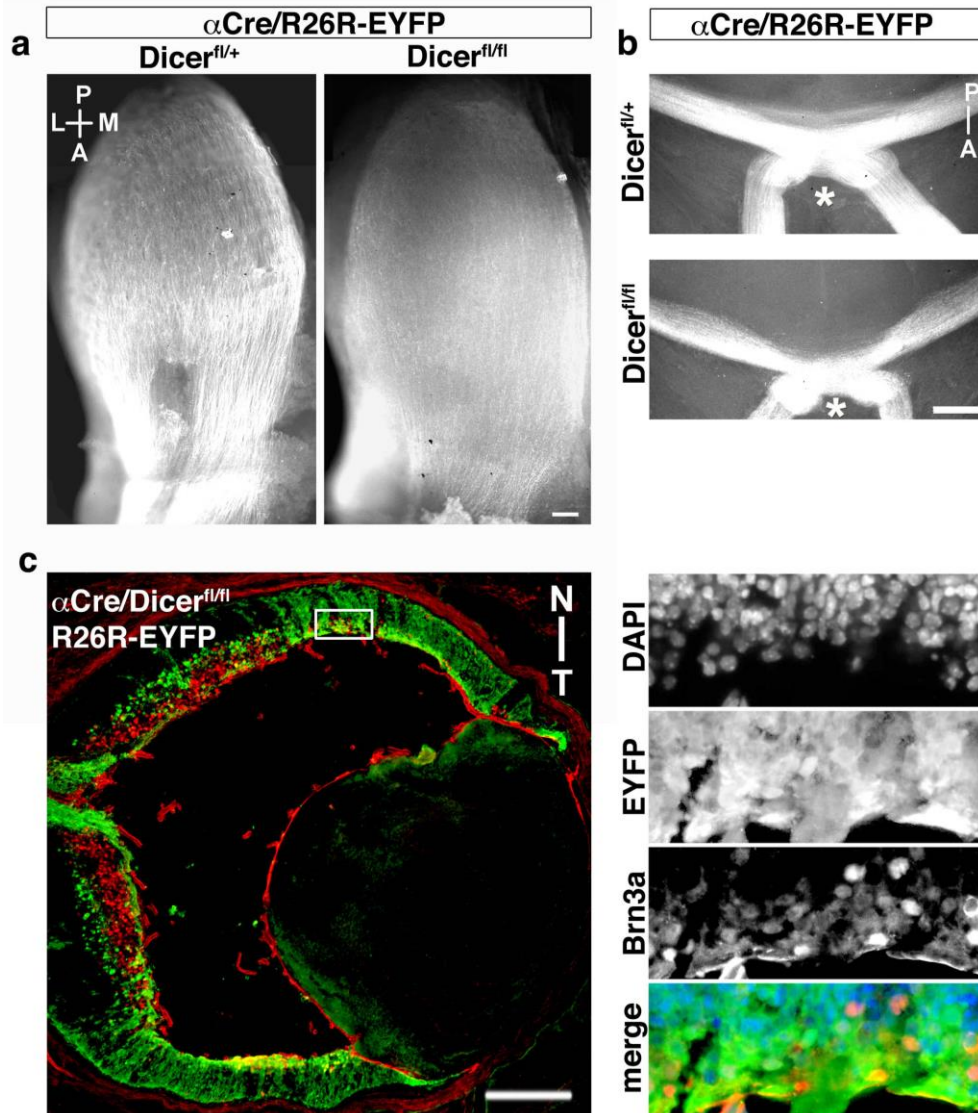


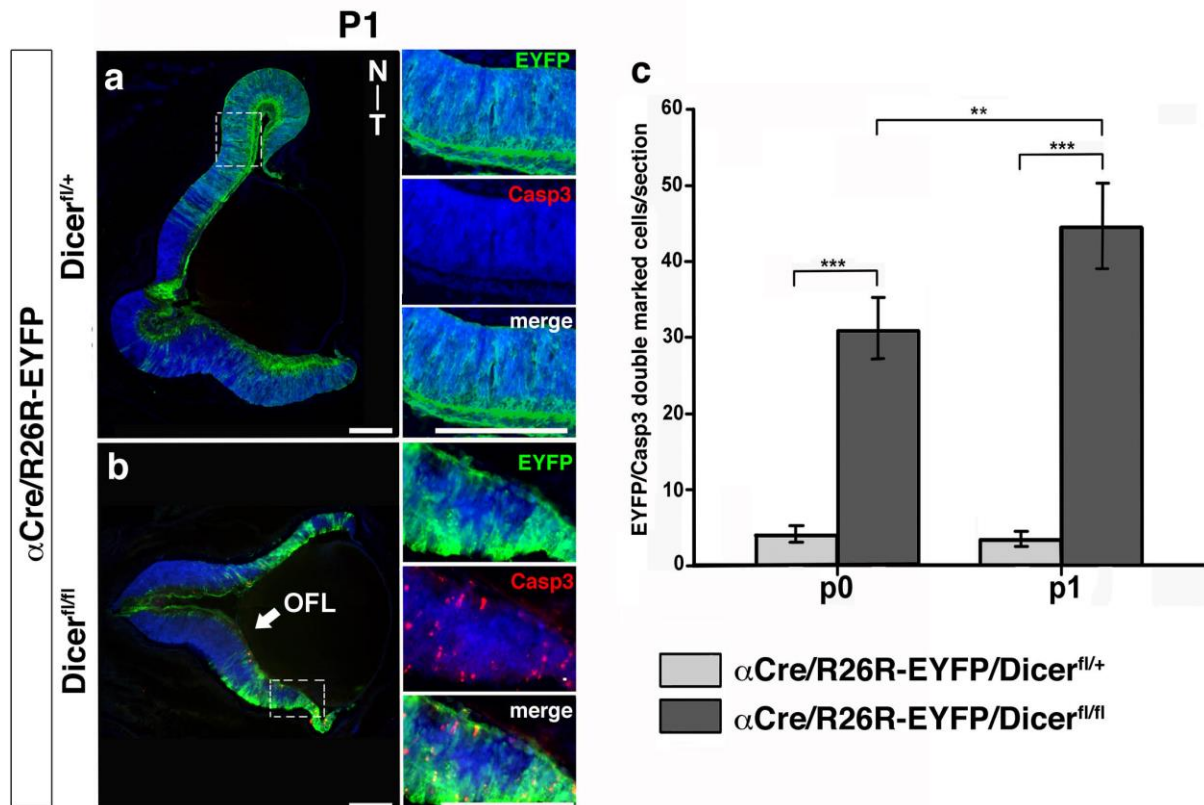
Supplementary Information

Restricted perinatal retinal degeneration induces retina reshaping and correlated structural rearrangement of the retinotopic map

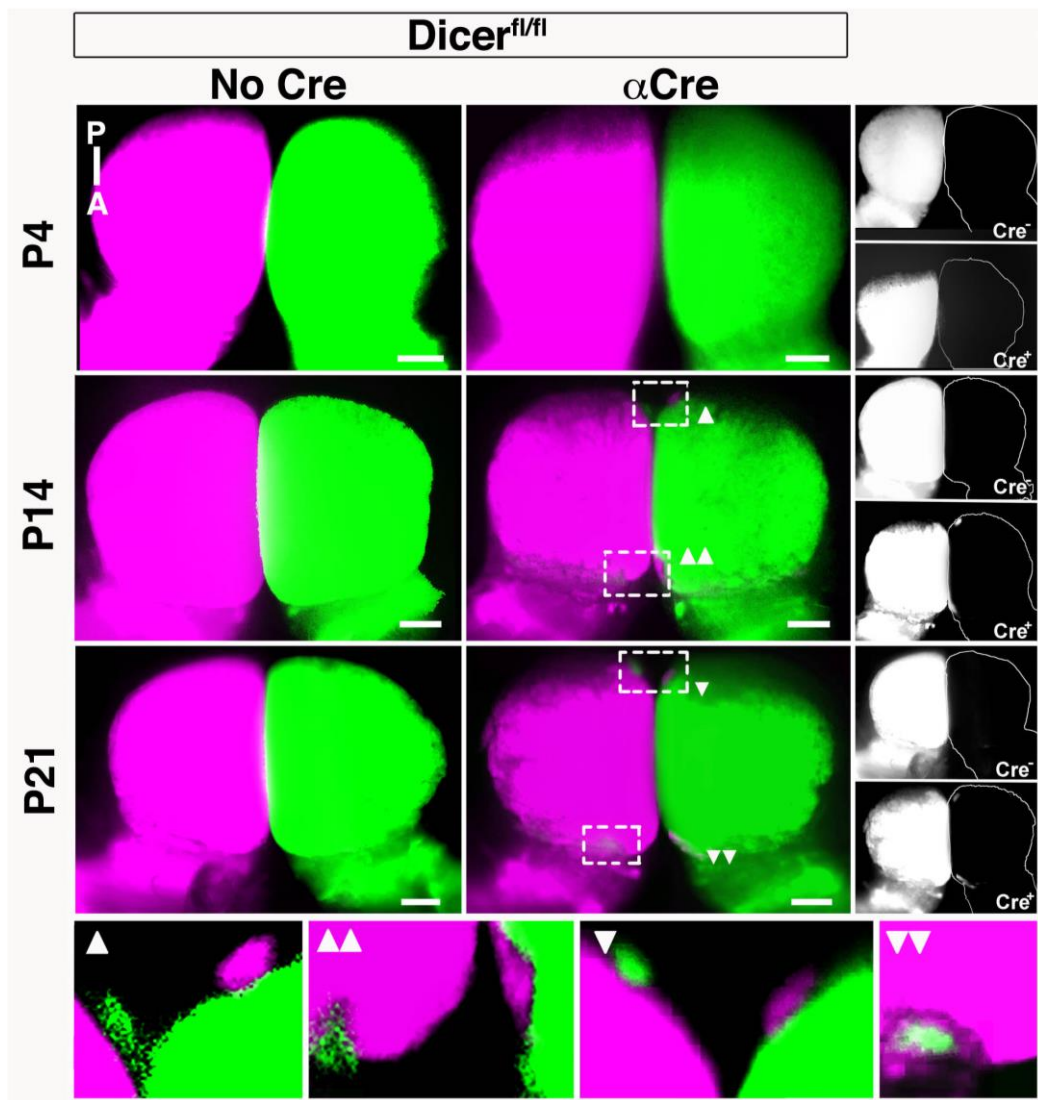
Nicola A. Maiorano and Robert Hindges



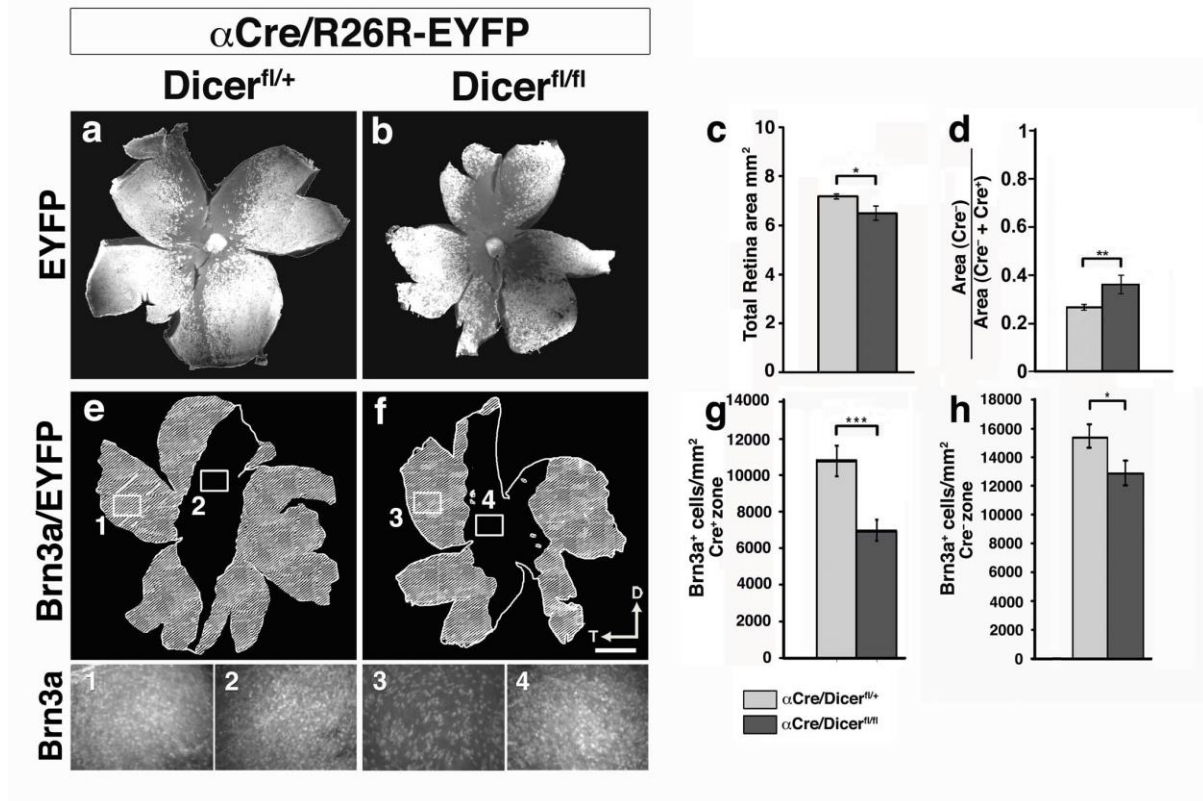
Supplementary Figure S1. Cre-positive RGC axons cross at the chiasm and reach the superior colliculus at early stages. **(a,b)** Whole mount immunohistochemical detection of EYFP to visualize axons from Cre-positive RGCs in heterozygous control (left) and homozygous floxed Dicer mice (right) at P0 in the superior colliculus (a) and at the chiasm (b). **(a)** EYFP positive RGC axons innervate the SC in both, control and Dicer1 mutant mice. **(b)** EYFP-positive RGC axons reach and decussate at the chiasm (asterisks) in both control and mutant mice. **(c)** Immunohistochemical detection of EYFP (green) and Brn3a (red) on P0 retina cryosections from Cre-positive, Dicer^{fl/fl} mice, counterstained with the nuclear marker DAPI (blue). Brn3a-positive ganglion cells are still present at P0 in peripheral retinae of mutant mice, although they fail to form a RGC layer. A, anterior; L, lateral; M, medial; N, Nasal; P, posterior; T, Temporal. Scale bars 50 μ m **(a)**, 100 μ m **(b)**, 200 μ m **(c)**.



Supplementary Figure S2 Deletion of Dicer1 in nasal and temporal retina leads to increased cell death and change in retinal morphology. **(a,b)** Cryosections from retina of control **(a)** and mutant **(b)** mice with subsequent immunohistochemical detection of EYFP (green) and Caspase 3 (red), counterstained with the nuclear marker DAPI (blue) at P1. In control mice almost no Caspase-positive cells can be detected **(a)** and retinal morphology looks normal. In contrast, high activation and nuclear localization of Casp3 is evident in Cre-positive retinal regions (EYFP-positive) of homozygous floxed Dicer mice, indicating increased cell death **(b)**. RGC axons from cre-positive nasal and temporal areas are still present in the optic fiber layer (OFL) **(c)** Quantification of Casp3-activated cells upon Cre-mediated deletion of Dicer1 in nasal and temporal retina at P1. EYFP/Caspase 3 double marked cells increase significantly in the mutant mice. Sample passed the Kolmogov-Smirnov for normality test. ANOVA followed by Bonferroni post-hoc test was applied. Values are mean \pm s.e.m. 5 sections for each different embryo (4 embryos for each test) were analyzed. ***P<0.001, **P<0.01. N, nasal; OFL optic fiber layer; T, temporal. Scale bars 200 μm .



Supplementary Figure S3 Genetic retinal lesions result in an extension of the remaining retinocollicular projections. Dorsal view of the SC at different postnatal stages of wild-type and α -Del mice after full eye fills with CTB-Alexa 488 (green) and -594 (magenta), similar to images shown in Fig. 2. In wild-type mice, both colliculi are filled completely with axon terminations from the contralateral eye at all stages. In contrast, mutant mice show poorly innervated posterior SC regions already at P4 (n=4 wild-type, n=3 α -Del). At P14 (n=6 wild-type, n=5 α -Del) and at P21 (n=3 wild-type, n=2 α -Del) empty SC areas are evident in anterior and posterior regions of the SC. Insets in P14 (triangles face-up) and P21 (triangles face-down) show patches formed by RGC terminations from the ipsilateral eye. Single channel images (Alexa-594) are shown on the right for increased contrast and signal detection. All images were adjusted for brightness and contrast. A, anterior; P, posterior. Scale bars 200 μ m.



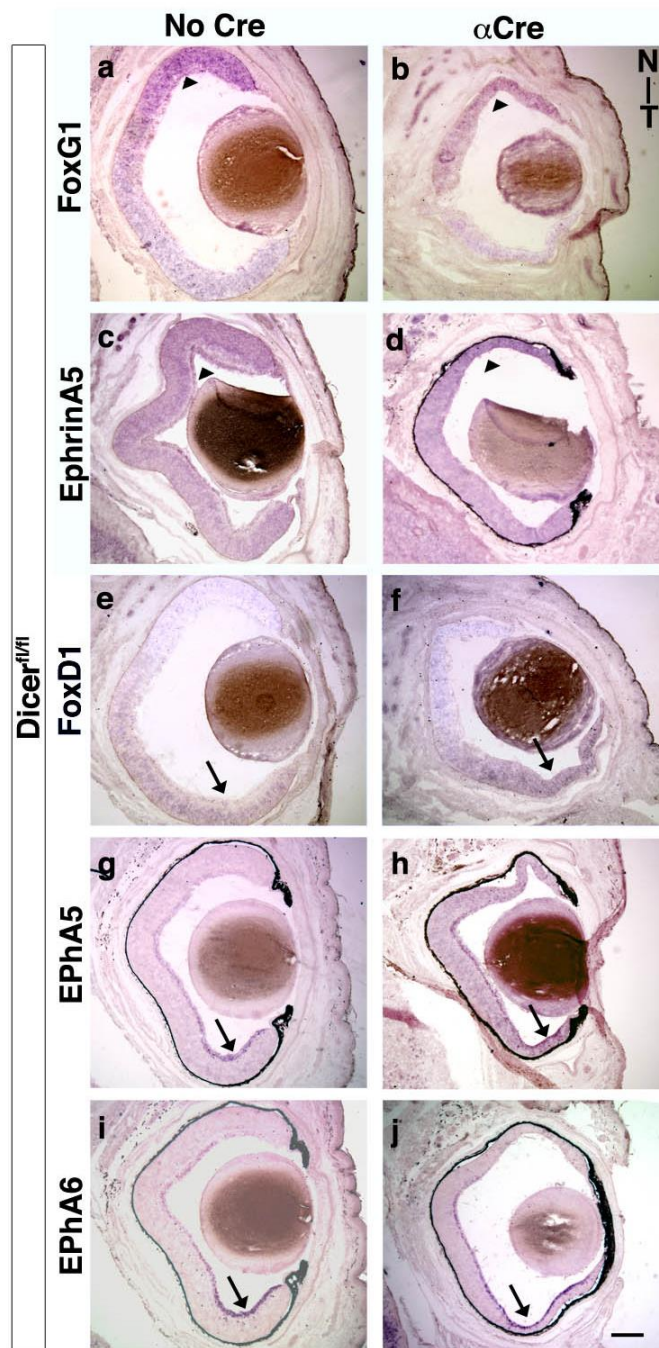
Supplementary Figure S4. Retinal changes are already apparent at birth

(a-d) Immunohistochemical detection of EYFP⁺ (Cre⁺) regions on retina flat mounts and quantifications in heterozygous controls **(a)** and homozygous mutant **(b)** animals at P0.

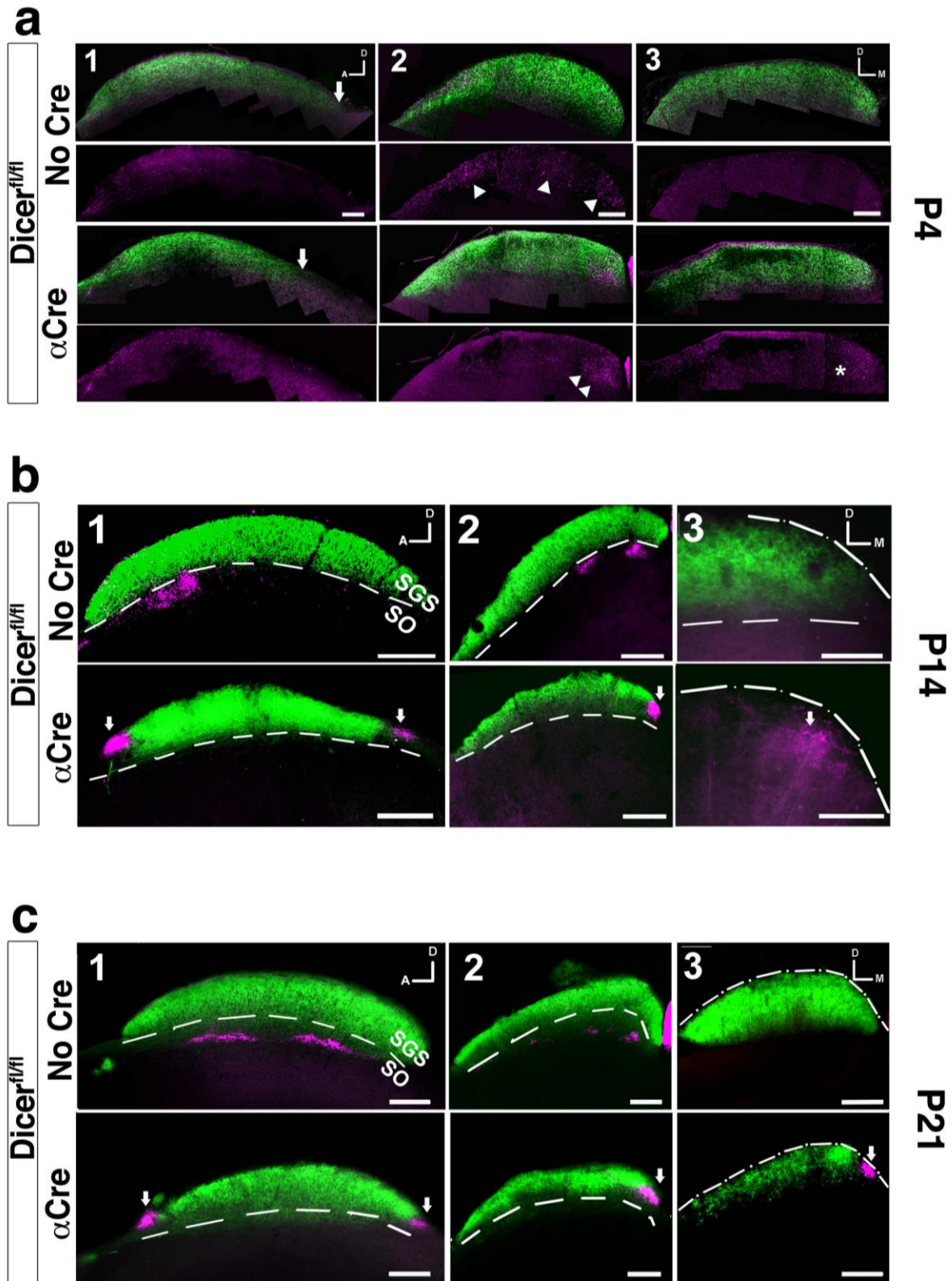
Mutant retinæ have already an enlarged Cre-negative domain compared to controls (2.4 ± 0.1 mm² vs 1.9 ± 0.1 mm² or $37 \pm 5\%$ vs $27 \pm 2\%$, respectively) despite a slight reduction in total retinal area (6.5 ± 0.3 mm² vs 7.2 ± 0.1 mm², respectively). Unpaired Student's t-test, 4 retinæ for each genotype analyzed.

(e-h) Immunohistochemical detection of Brn3a-positive cells in retinæ from mutant and heterozygous control mice at P0. Insets illustrate Brn3a-positive cells in central (2, 4) Cre-negative (EYFP⁻) and peripheral (1, 3) Cre-positive retina (EYFP⁺) as shown in the camera lucida schematics. At this stage, a significant number of RGCs (Brn3a positive) is still present in the Cre-positive zone of α -Del mutant retina (inset 3).

(g-h) Density quantification of Brn3a-positive cells for both genotypes in the Cre-negative and positive zones. Unpaired Student's t-test, 4 retinæ for each genotype analyzed (see methods section for more details). Values are mean \pm s.e.m. ***P<0.001, **P<0.01, *P<0.05. D, dorsal; T, temporal. Scale bar 500 μ m (a, b, e, f).

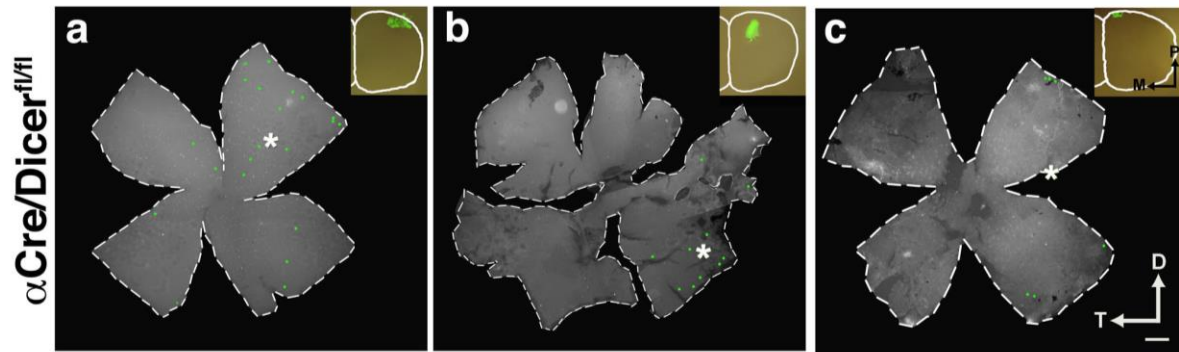


Supplementary Figure S5 Expression of molecular markers along the nasal-temporal retinal axis is unchanged in mutant mice. (a-j) Panels show *in situ* hybridization on horizontal retinal sections using specific riboprobes against nasal (*FoxG1*, *Ephrin-A5*, arrowheads) and temporal (*FoxD1*, *EphA5*, *EphA6*, arrows) markers. In all cases, expression gradients are conserved in mutant retinæ (α Cre), compared to tissues from wild-type littermates (no Cre). N, nasal; T, temporal. Scale bar 200 μ m.

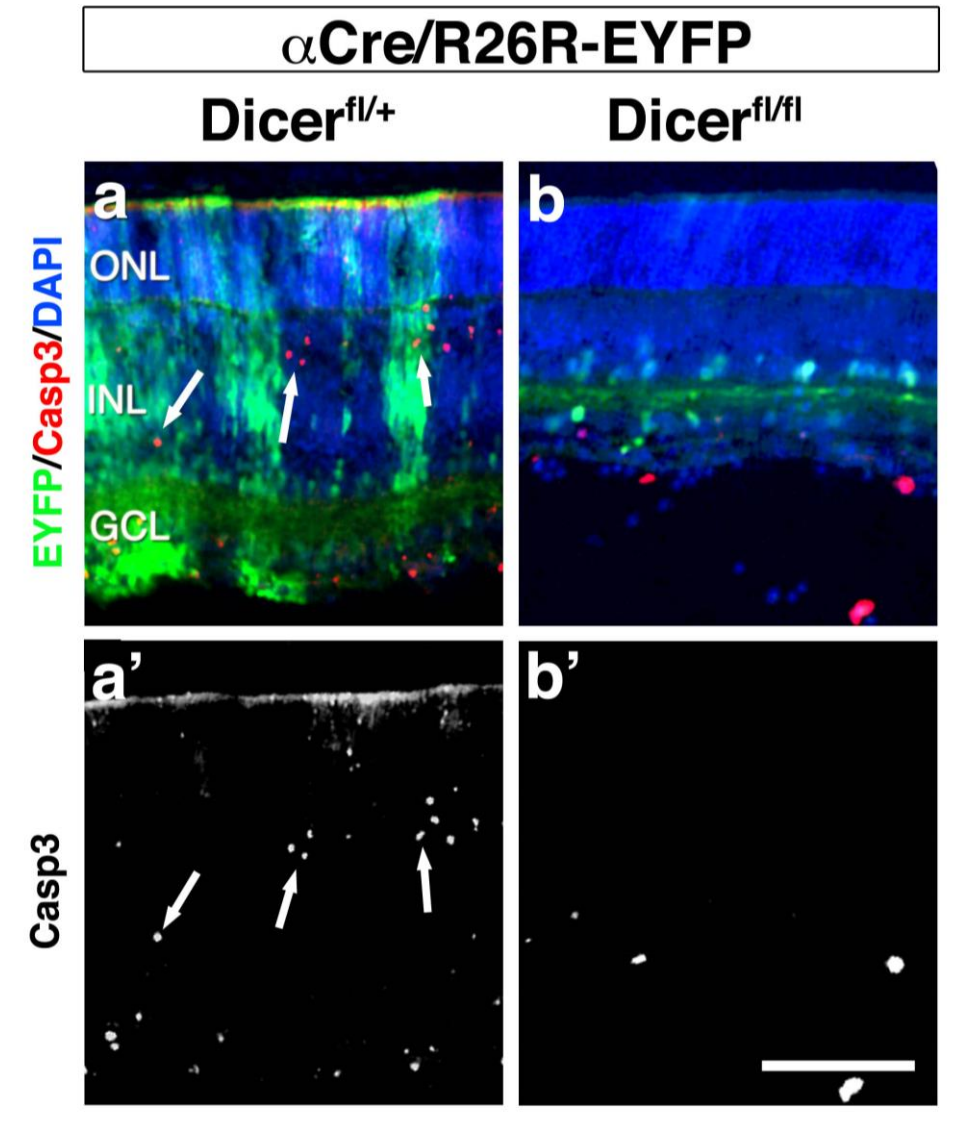


Supplementary Figure S6 Aberrant projections from ipsilateral RGCs are formed during early postnatal stages and remain stable after eye opening. **(a-c)** Sections through the SC of wild-type (upper panels) and α -Del mutant mice (lower panels) after full eye fills with CTB Alexa 488 (green, contralateral eye) and CTB Alexa 594 (magenta, ipsilateral eye) at three different postnatal stages. **(a)** Parasagittal sections of the SC at P4 (1) show the diffuse

innervation by ipsilateral RGC axons (red) in wild-type and α -Del mutant mice. Contralateral RGC axons (green) are extending to the posterior SC border in wild-type mice, in contrast to axons in α -Del mice that stop more anteriorly (arrows). Anterior coronal sections (**2**) illustrate ipsilateral RGC axons (magenta) spread across the medial-lateral width of the SC in wild-type mice, whereas ipsilateral RGC axons already cluster in the medial SC in mutant mice (arrowheads). Similarly ipsilateral RGC axons were present in the posterior SC in α -Del mice (**3**), clustering in the medial zone (asterisk). (**b,c**) At P14 and after eye opening at P21, in wild-type mice the ipsilateral projections (magenta) terminate discontinuously in only anterior positions of the stratum opticum (SO) below the dorsal-most stratum griseum superficiale (SGS), which is occupied by contralateral projections (green). In mutant mice, two completely segregated termination zones of ipsilateral RGC axons are found in the anterior and posterior SC (arrows). In addition, the terminations are not confined to the deeper SO, but are located incorrectly in the SGS. Dashed lines indicate border between SGS and SO, dashed-dotted lines indicate the dorsal SC border in (**3**). For all genotypes n=3 (P4), n=3 (P14) and n=2 (P21). A, anterior; D, dorsal; M, medial. Scale bars 200 μ m.



Supplementary Figure S7 Nasal RGC axons project to the posterior ipsilateral SC in $\alpha\text{-Del}$ mutant mice. (**a-c**) Whole retina flatmounts detecting RGCs after retrograde labeling using fluorescent microbeads injected in the posterior ipsilateral SC (see insets) of lesion-induced mutant mice at P8. Asterisks illustrate the center of mass of labeled RGCs calculated as the average position in the x- and y-axis of the retinae (nasal-temporal and dorso-ventral respectively). In all cases analyzed, the retrogradely labeled RGCs are located in nasal retina. D, dorsal; M, medial; P, posterior; T, temporal temporal-dorsal. Scale bar 300 μm .



Supplementary Figure S8 General retinal cell death is decreased in α -Del mice. **(a,b)** Retinal cryosections and subsequent immunohistochemical detection of EYFP (green) and Caspase 3 (red), counterstained with DAPI in heterozygous control mice (a) and homozygous mutant mice (b) at P8. **(a,a')** In control animals, apoptotic cells (arrowheads) are detected across the retinal layers in both Cre-positive and -negative domains (n=3). **(b,b')** In contrast, in α -Del mutant mice most of the Cre-positive nasal and temporal areas have disappeared and the remaining retinal tissue shows only very few apoptotic cells at this late stage (n=3). The remaining EYFP-positive cells in **(b)** are a subset amacrine cells, in which the α Pax6 promoter element is activated after cell differentiation and that are not undergoing cell death. (GCL, ganglion cell layer; INL, inner nuclear layer; ONL, outer nuclear layer). Scale 200 μ m.